JOURNAL OF MAGNETIC RESONANCE 98, 134–141 (1992)

Effects of Higher-Rank Multipoles on Spectral Lineshapes of $I = \frac{3}{2}$ Quadrupolar Nuclei Near the Null Point in Inversion-Recovery Experiments

WILLIAM S. PRICE, NIEN-HUI GE, AND LIAN-PIN HWANG*

Department of Chemistry, National Taiwan University, Taipei, Taiwan, Republic of China; and Institute of Atomic and Molecular Sciences, Academia Sinica, Taipei, Taiwan, Republic of China

Received September 17, 1991

The effects of higher-rank multipoles on the spectral lineshape of $I = \frac{3}{2}$ quadrupolar nuclei have been examined near the null point in inversion-recovery measurements. ^{7}Li NMR inversion-recovery experiments were performed on LiCl dissolved in isopropanol-d_8/D_2O solution at 225 K. The state multipole formalism approach was applied to interpret relaxation processes and analyze lineshapes. The experimental spectra could be simulated using a correlation time of 1.1 ns for the fluctuation of the direction of the electric field gradient at the ^{7}Li nucleus and a quadrupolar coupling constant of 42.7 kHz. The excellent agreements between observed and simulated spectra demonstrate that analysis of spectral lineshapes derived from inversion-recovery experiments provides a convenient way of determining the quadrupolar coupling constant and the fluctuation correlation time of the electric field gradient at the nucleus and of observing the dynamic frequency shift.

In a recent study, it was demonstrated theoretically that, for quadrupolar nuclei in the nonmotional narrowing region, the effects of the higher-rank multipoles (rank $\geqslant 3$) may be generated after the spin inversion in the $180° — \tau — \theta$ pulse experiment (*1, 2*). Although the calculated NMR lineshape is dependent on τ and θ, the effects are normally not observed due to the small deviation from the lineshape obtained if the system was in thermal equilibrium before the detection pulse. Furthermore, the spectral lineshapes obtained in the inversion-recovery experiment are usually identical to those resulting from a 90° pulse applied to the spin system in thermal equilibrium.

It has been shown previously that, in the usual inversion-recovery experiments, the relaxations of dipole–dipole cross interactions and their associated third rank multipole of the three methyl protons in $Co(acac)_3$ solution may be revealed from studies of the spectral lineshape near the null point (*3*). The lineshape so obtained is significantly different from that obtained after application of a 90° pulse to a spin system in equilibrium. Here, we demonstrate that a similar technique may be used to exhibit the effects of higher-order multipoles in quadrupolar relaxation. We have again used the state multipole approach (*4*) to simplify the formulation of the relaxation processes. In the present study we chose the comparatively simple system of lithium chloride dissolved in isopropanol-d_8/D_2O solution.

* To whom correspondence should be addressed.

0022-2364/92 $5.00

TABLE 1

Relaxation Matrices $\mathbf{R}_l$ and $\mathbf{R}_t$ for the Quadrupole Interaction on Resonance, for Quadrupolar Nuclei with Spin Quantum Number = $\frac{3}{2}$: The Notation Follows That of Einarsson and Westlund (*2*)[a,b,c]

$$\mathbf{R}_{l,t} = \mathrm{K} \cdot \begin{bmatrix} A & C \\ C & B \end{bmatrix}; \qquad \mathrm{K} \equiv \frac{1}{30}\left(\frac{eQ}{\hbar}\right)^2$$

	Longitudinal	Transverse
A	$2J_1 + 8J_2$	$3J_0 + 5J_1 + 2J_2 - iQ_1 - 2iQ_2$
B	$8J_1 + 2J_2$	$2J_0 + 5J_1 + 3J_2 + iQ_1 - 3iQ_2$
C	$4(J_1 - J_2)$	$\sqrt{6}\,(J_0 - J_2 - 2iQ_1 + iQ_2)$

[a] There are some misprints in the coefficients and signs in Ref. (*2*) and these have been corrected here.

[b] The fluctuation of the electric field gradient in the quadrupolar relaxation mechanism is assumed to change in direction but not magnitude.

[c] The equilibrium values for the longitudinal state multipoles are $\sigma_0^1 = \sqrt{5}\,\gamma_I\,\hbar\,B_0/(2I+1)\,kT$ and $\sigma_0^3 = 0$, where B_0 is the magnetic field.

Normally the spectra obtained from quadrupolar nuclei, in the nonmotional narrowing region, have structureless Lorentzian-like lineshapes. This study demonstrates that analysis of the fine spectral structure observed near the null point provides a more reliable means for determining the quadrupolar coupling constant and the fluctuation correlation time of the electric field gradient at the nucleus (τ_c) than attempts to interpret multiexponential relaxation data. This method also provides a convenient means of observing the dynamic frequency shift.

THEORY

The time evolution of the spin-density matrix is calculated using the Redfield equation (*5*). Following earlier studies (*1, 2*), the relaxation equation is simplified by expressing it in a basis in which the individual elements of the density matrix transform as components of the full rotation group. The new elements, σ_m^k, of the density matrix are state multipoles (*4*), where the superscript k represents the rank and the subscript m represents the tensorial component of the state multipole. The longitudinal and transverse magnetizations are determined by σ_0^1 and σ_1^1 (or σ_{-1}^1), respectively.

The state multiple equation of motion for longitudinal relaxation may be expressed by

$$\frac{d}{dt}\begin{bmatrix} \sigma_0^1 \\ \sigma_0^3 \end{bmatrix} = -\,\mathbf{R}_l \begin{bmatrix} \sigma_0^1 \\ \sigma_0^3 \end{bmatrix}, \qquad [1]$$

where $\mathbf{R}_l$ is the relaxation matrix for the longitudinal components of the state multipoles. The relaxation matrices for quadrupolar relaxation, including second-order

dynamic frequency shifts, previously derived by Einarsson and Westlund (*2*), have been corrected and is given in Table 1.

The description of the relaxation processes following the inversion-recovery pulse sequence is given in terms of the evolution of the state multipoles. In order for the longitudinal components of the state multipoles to achieve thermal equilibrium values at infinite time, we substitute the difference between σ_0^k and its equilibrium distribution value for σ_0^k in Eq. [1]. Further, the evolution of the longitudinal/transverse state multipole components conserves parity (e.g., if the spin system initially contains non-zero longitudinal/transverse components of odd rank then no even rank longitudinal/transverse components will couple with odd rank components during evolution).

An on-resonance radiofrequency pulse transforms the state multipole components according to the relation (*6*)

$$(\sigma^+)_m^k = \sum_n D_{mn}^k(\phi - \pi/2, \theta, \pi/2 - \phi)(\sigma^-)_n^k, \qquad [2]$$

where D_{mn}^k is a Wigner rotation matrix element (*7*), θ is the radiofrequency pulse angle, ϕ is the radiofrequency phase angle with respect to the x axis in the rotating frame, and the superscripts $+/-$ indicate the state multipole components after/before the pulse. Thus, after the $\pi/2$ monitor pulse ($\phi = \pi/2$ and $\theta = \pi/2$) and in the acquisition period, the state multipoles related to the single-quantum coherences at Larmor frequency, ω_0, may be evaluated from

$$\frac{d}{dt}\begin{bmatrix}\sigma_1^1\\ \sigma_1^3\end{bmatrix} = (-\mathbf{R}_t - i\omega_0\mathbf{I})\begin{bmatrix}\sigma_1^1\\ \sigma_1^3\end{bmatrix}, \qquad [3]$$

where $\mathbf{I}$ is the unit matrix and $\mathbf{R}_t$ is the relaxation matrix for the transverse components of the state multipoles. The elements of $\mathbf{R}_t$ for quadrupolar relaxation are defined in Table 1.

Starting from thermal equilibrium, Eq. [1] is used to follow the evolution of the longitudinal magnetization during the τ delay between the 180° and 90° pulses in the inversion-recovery sequence. Equation [2] is then applied to account for the effects of the 90° pulse and the result forms the initial condition for calculating the transverse evolution during the acquisition period using Eq. [3]. The spectral lineshape is related to the real part of the Fourier–Laplace transform of the σ_1^1 term, which evolves during the acquisition period.

EXPERIMENTAL

LiCl was obtained from Merck (Darmstadt, Germany). Isopropanol-d_8 (99+ at% D) was from Janssen Chimica (Geel, Belgium). D_2O (99.9%) was obtained from Isotec (OH). In preparing the samples the appropriate amount of LiCl was mixed with isopropanol-d_8 and D_2O in a 5 mm o.d. NMR tube to give a solution (~0.27 ml) containing 0.2 *M* LiCl and 9 *M* D_2O. The solution was then degassed by five freeze–thaw cycles. The tube was then flame sealed. The ^{7}Li NMR measurements were performed using a Bruker MSL-300 spectrometer operating at 116.64 MHz. The field homogeneity was carefully adjusted and the temperature was controlled at 225 ± 0.5 K. Typical acquisition parameters were a spectral width of 1000 Hz digitized

into 4K data points with a $\pi/2$ pulse length of 23 μs. The near null point spectra were obtained using the inversion-recovery pulse sequence. The T_2 measurements were obtained using the Hahn spin-echo pulse sequence. A delay of at least $5T_1$ was allowed between scans for T_2 measurements and at least $10T_1$ for the null point spectra.

RESULTS AND DISCUSSION

Experimental and simulated ^{7}Li null point spectra corresponding to various τ delay times in the inversion-recovery pulse sequence are shown in Fig. 1. The fine structure in the null point spectra becomes apparent at an inversion-recovery delay of 250 ms as a small nick in the high-field side of the inverted resonance. With increasing τ, the

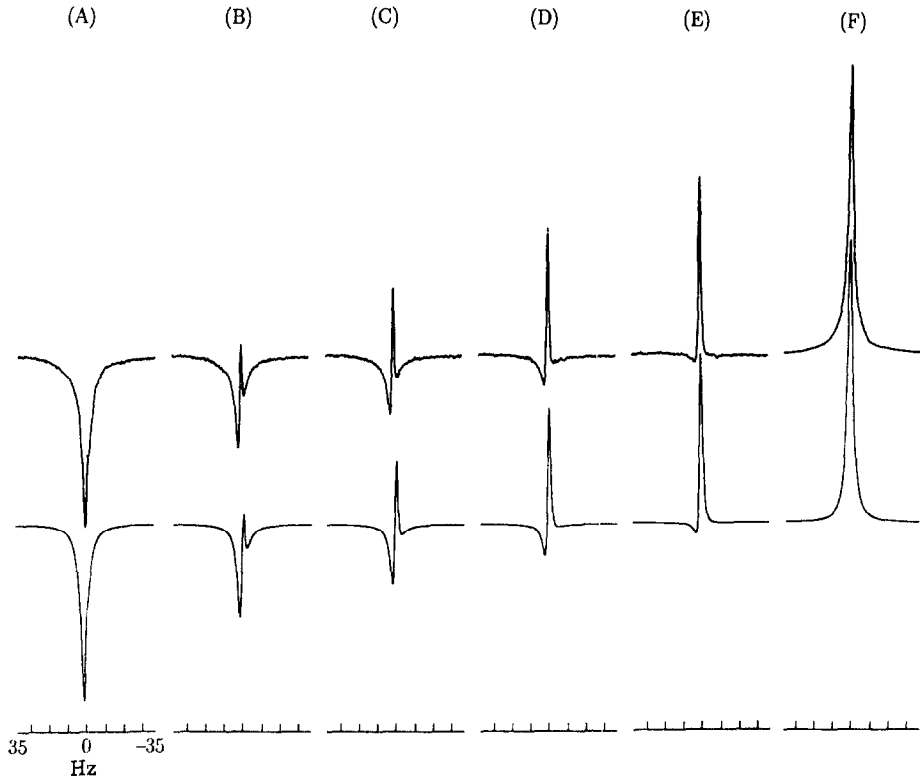

FIG. 1. Experimental (top) and simulated (bottom) ^{7}Li inversion-recovery spectra as a function of the τ delay time. The observed linewidth at half-height of the spectrum obtained when the τ delay was sufficient to ensure that the system was in thermal equilibrium before the detection pulse was applied was 3.0 Hz. The experimental spectra are presented with 0.2 Hz of line broadening. The simulated spectra have 1.4 Hz of line broadening added to account for unspecified transverse relaxation, mainly magnetic inhomogeneity. The τ values and the ordinate magnifying factors for the spectra are given respectively by (A) 250 ms, 16; (B) 260 ms, 16; (C) 265 ms, 16; (D) 270 ms, 16; (E) 275 ms, 16; (F) 4 s, 1. From the spectra it can be seen that the minimum intensity in the inversion-recovery experiment occurs at 260 ms and that before about 250 ms and after 275 ms no fine structure is visible in the spectra. The fine structure visible near the null point is a consequence of the evolution of the rank 3 multipole. The asymmetry in the near null point spectra results from the dynamic frequency shift.

nick enlarges and relaxes faster to the upright position. The fine structure in the spectrum disappears when the τ value exceeds 280 ms. Were the period over which the fine structure was observable too short, then it would not be possible to analyze the spectra reliably. Relative to the intensity of the spectrum obtained when the τ delay is sufficient to allow for full longitudinal relaxation, the null point spectra are about 16 times smaller.

Excellent agreement between experimental and simulated null point spectra was obtained by using a quadrupolar coupling constant of 42.7 kHz and a value of 1.1 ns for τ_c. This value of τ_c corresponds to $\omega\tau_c = 0.83$. The apparent T_2 value of 197 ms, derived by regressing a single exponential onto the spin-echo data, gave an intrinsic linewidth at half-height of 1.6 Hz. This value was the same as the linewidth at half-height obtained from our simulation of the fully relaxed spectrum. The value of 42.7 kHz for the quadrupolar coupling constant is close to the value of 39.5 kHz obtained from Monte Carlo simulations for dilute Li in aqueous solutions (*8*). In the Monte Carlo simulations, the Monte Carlo "box" was a hard sphere with the ion at its center. The ion was surrounded by 50 rigid water molecules. The similarity between the two coupling constants implies that lithium dissolved in isopropanol-d_8/D_2O is in an environment similar to that of lithium dissolved in water.

In reality there is a minor dipole–dipole contribution to the ^{7}Li relaxation. The relevant relaxation matrix elements are given in the Appendix. In accounting for the dipole–dipole contribution to the lithium ion it was assumed that the fluctuation correlation time for the dipole–dipole interaction was the same as the fluctuation correlation time for the electric field gradient at the nucleus. It was also assumed that the first hydration sphere was composed of 5.5 water molecules, with the average Li to D distance being 2.55 Å as determined from neutron scattering data (*9*). If the dipole–dipole contribution is included, the null point spectra can be simulated with

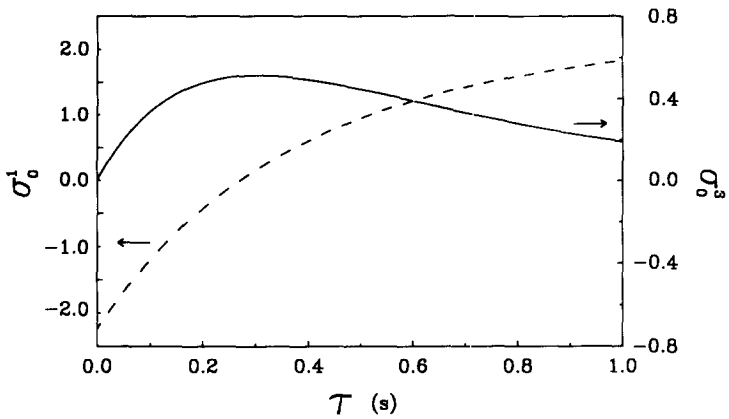

FIG. 2. A plot of the time evolution during the τ delay of the inversion-recovery sequence of the rank 1 (σ_0^1, ---) and rank 3 (σ_0^3, —) longitudinal state multipoles. The scale of the rank 3 multipole has been enlarged relative to that of the rank 1 multipole to enable the difference in the evolutions to be clearly seen. The plot shows that the maximum value for the rank 3 multipole occurs at approximately the same time as the minimum absolute signal amplitude in the inversion-recovery experiment. The ordinate scale is in units of $\gamma_I \hbar B_0/(2I + 1)\,kT$.

τ_c = 1.2 ns and a quadrupolar coupling constant of 42.0 kHz, with the dipole–dipole contribution accounting for 4.7% of the total ^{7}Li longitudinal relaxation.

The fine spectral structure observed near the null point (See Fig. 1) clearly shows the truly double exponential nature of the relaxation processes. In the T_2 measurement, however, the double exponential nature of the relaxation was not clear and the relaxation curve was well described by a single exponential.

The variations of rank 1 and 3 state multipoles with different inversion delay times (i.e., τ) are shown in Fig. 2. The σ_0^1 curve corresponds to the inversion-recovery process of the longitudinal magnetization. Near the null point of σ_0^1, σ_0^3 reaches its maximum value and the effects of its coupling with σ_0^1 is apparent as the fine structure observed in the spectra.

The imaginary parts of the relaxation matrix (i.e., Q_1 and Q_2, referred to in Table 1) give the dynamic frequency shift. Since the Q_1 and Q_2 terms vary according to $\omega\tau_c/[1 + (\omega\tau_c)^2]$, the dynamic frequency shift vanishes when $\omega\tau_c \ll 1$ or $\omega\tau_c \gg 1$. The resultant effects on spectral lineshapes are demonstrated in Fig. 3. When $\omega\tau_c \approx 1$ the fine structure of the null point spectrum is most visible and experimentally accessible. If $|\mathcal{H}_Q\ \tau_c|$ is not much smaller than 1, where $\mathcal{H}_Q$ is the quadrupolar Hamiltonian, then second-order perturbation theory does not hold and higher-order perturbations need to be considered. This can be performed by a minor modification of the stochastic Liouville equation approach of Hwang and Ju (*10*).

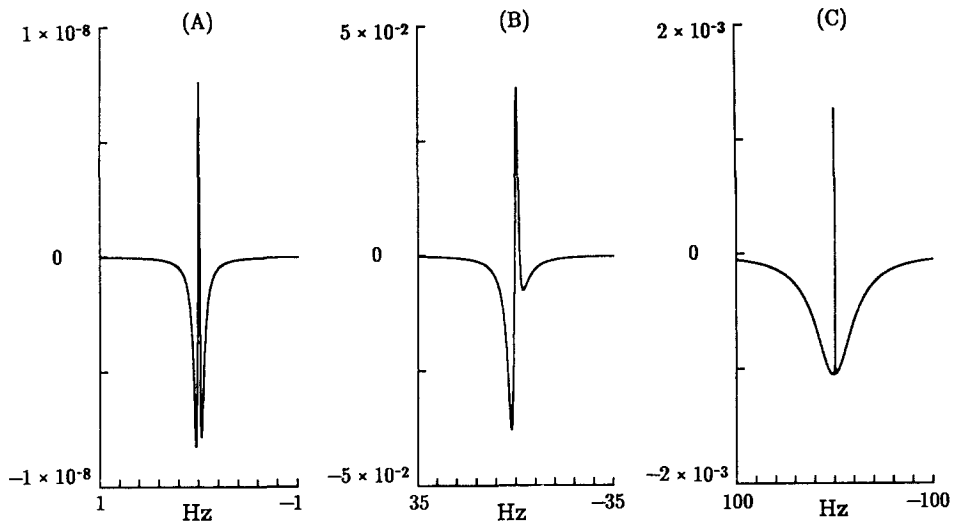

FIG. 3. Plots of simulated spectral lineshapes for ^{7}Li near the null point in an inversion-recovery experiment. The simulations were performed with a quadrupole coupling constant of 42.7 kHz and various values for τ_c and of inversion-recovery τ delays: (A) τ_c = 20 ps, τ = 4.818 s, $\omega\tau_c$ = 0.02; (B) τ_c = 1.37 ns, τ = 275 ms, $\omega\tau_c$ = 1.00; and (C) τ_c = 40 ns, τ = 3.867 s, $\omega\tau_c$ = 29.32. The ordinate shows the intensity of each spectrum relative to its corresponding fully relaxed spectrum. It should be noted that the duration of τ for which the fine structure is visible increases with increasing τ_c. In simulating (A) the fine structure was visible for less than 1 μs. The simulated spectra clearly show the $\omega\tau_c$ dependence of the assymmetry of the dynamic frequency shift.

This study shows that the observation of higher-rank multipole effects in inversion-recovery experiments of quadrupolar nuclei in the nonmotional narrowing region and subsequent analysis using the state multipole formalism provide a powerful technique for determining τ_c and the quadrupolar coupling constant. This method obviates the need to perform (unreliable) multiexponential regressions on relaxation data. Continuing work in this laboratory is aimed at applying this method to quadrupolar nuclei with higher spin quantum numbers and at assessing the use of these methods for studying quadrupolar systems in the presence of chemical exchange.

APPENDIX

State Multipole Formulation for the Dipole–Dipole Interaction Contribution to ^{7}Li Relaxation

In the present work it has been assumed that the dipole–dipole contribution to ^{7}Li relaxation results exclusively from the first hydration sphere. The state multipole relaxation matrices for longitudinal and transverse relaxation are given by

$$\mathbf{R}_1 = \begin{bmatrix} 2j_1 & 0 \\ 0 & 12j_1 \end{bmatrix}$$

and

$$\mathbf{R}_t = \begin{bmatrix} j_0 + j_1 - iq_1 & 0 \\ 0 & j_0 + 11j_1 - iq_1 \end{bmatrix},$$

respectively. The terms j_0, j_1, and I_1 are defined by

$$j_0 = \frac{1}{15} N_D S(S+1)(\gamma_I \gamma_S \hbar)^2 \left\langle \frac{1}{r^6} \right\rangle \{3J(\omega_S) + 2J(0)\},$$

$$j_1 = \frac{1}{10} N_D S(S+1)(\gamma_I \gamma_S \hbar)^2 \left\langle \frac{1}{r^6} \right\rangle \{J(\omega_I) + 2J(\omega_I + \omega_S) + \frac{1}{3} J(\omega_I - \omega_S)\},$$

and

$$q_1 = \frac{1}{10} N_D S(S+1)(\gamma_I \gamma_S \hbar)^2 \left\langle \frac{1}{r^6} \right\rangle \{Q(\omega_I) + 2Q(\omega_I + \omega_S) + \frac{1}{3} Q(\omega_I - \omega_S)\},$$

where N_D is the number of deuterium nuclei in the first hydration sphere of the Li nucleus, S is the deuteron spin quantum number, γ_I is the ^{7}Li magnetogyric ratio, γ_S is the D magnetogyric ratio, r is the Li-to-D distance, the angled brackets denote the equilibrium average, $\hbar$ is Planck's constant, and ω_I and ω_S are the ^{7}Li and D Larmor frequencies, respectively. The spectral densities are defined by

$$J(\omega) \equiv \frac{2\tau_0}{1 + (\omega\tau_0)^2}$$

$$Q(\omega) \equiv \omega\tau_0 J(\omega),$$

where τ_0 is the fluctuation correlation time for the dipole–dipole interaction. The fluctuation of the dipole–dipole interaction is assumed to be an exponentially decaying process,

$$\left\langle \frac{D^2_{0m}(\Omega_t) D^2_{0m}(\Omega_0)^*}{r_t^3 r_0^3} \right\rangle = \frac{1}{5} \left\langle \frac{1}{r^6} \right\rangle e^{-t/\tau_0},$$

where Ω_0 and Ω_t are the Euler angles defining the orientation of the lithium-to-deuterium direction vector at times 0 and t, respectively, and r_0 and r_t are the distance between the lithium and deuterium nuclei at times 0 and t, respectively.

ACKNOWLEDGMENT

Support of this work by grants from the National Science Council of the Republic of China is gratefully acknowledged.

REFERENCES

1. P. O. WESTLUND AND H. WENNERSTRÖM, *J. Magn. Reson.* **50,** 451 (1982).
2. L. EINARSSON AND P. O. WESTLUND, *J. Magn. Reson.* **79,** 54 (1988).
3. T. S. LEE AND L. P. HWANG, *J. Magn. Reson.* **89,** 51 (1990).
4. B. C. SANCTUARY, *J. Magn. Reson.* **61,** 116 (1985) and pertinent references therein.
5. A. G. REDFIELD, *in* "Advances in Magnetic Resonance" (J. S. Waugh, Ed.), Vol. 1, p. 1, Academic Press, San Diego, 1965.
6. I. FURÓ, B. HALLE, AND T. C. WONG, *J. Chem. Phys.* **89,** 5382 (1988).
7. D. M. BRINK AND G. R. SATCHLER, "Angular Momentum," Oxford Univ. Press, London, 1968.
8. S. ENGSTRÖM, B. JÖNSSON, AND B. JÖNSSON, *J. Magn. Reson.* **50,** 1 (1982).
9. J. E. ENDERBY AND G. W. NEILSON, *Adv. Phys.* **29,** 323 (1980).
10. L. P. HWANG AND C. Y. JU, *J. Chem. Phys.* **83,** 3775 (1985).